Xiaoxianxiong Decoction Ameliorates Obesity-induced Type 2 Diabetes by Suppressing the NLRP3 Inflammasome Activation

Ruqian Ding[1], Yihan Wang[2], Yijiu Yang[3], Zhenhua Zhang[1]*

[1]Guang'anmen Hospital, China Academy of Chinese Medical Sciences, Beijing 100053, China

[2]National Research Institute for Family Planning, Beijing 100081, China

[3]Institute of Basic Research in Clinical Medicine, China Academy of Chinese Medical Sciences, Beijing 100700, China

***Corresponding author:**

Zhenhua Zhang, Ph.D,

Guang'anmen Hospital, China Academy of Chinese Medical Sciences, Beijing 100053, China,

Tel: (86) 10-8280-5570, Fax: (86) 10-8280-1380,

E-mail: katiezhang606729@126.com

Received : April 02, 2026

Published : May 28, 2026

ABSTRACT

Obesity leads to chronic and systemic inflammation, resulting in insulin resistance (IR) and type 2 diabetes (T2D). This chronic inflammation has emerged as a key feature of T2D. Xiaoxianxiong decoction (XXXD) is a classic and well-known decoction that has been used to treat patients with severe pneumonia by inhibiting the inflammatory response. However, the pharmacological mechanism underlying XXXD ameliorates obesity-induced T2D is poorly understood. Here, we demonstrated that XXXD alleviated T2D by suppressing the inflammation through the NLRP3-dependent pathway. We found that XXXD-treated mice had significantly lower blood glucose levels and body weights in the HFD + STZ mouse model (Streptozotocin with high-fat diet). XXXD improved insulin resistance (IR) as indicated by the Oral glucose tolerance test (OGTT) and the insulin tolerance test (ITT) analyses. Oil red O staining and hematoxylin and eosin (H&E) staining showed that XXXD protected against the development of hepatic steatosis in the T2D mice model. Mechanistically, XXXD reduced hepatic inflammation through the NLRP3-mediated signaling pathway. In addition, we demonstrated that XXXD inhibited the accumulation of macrophages and their transformation into a pro-inflammatory state in the T2D livers. Through molecular docking simulation and molecular dynamics (MD) simulations, we identified the glucocorticoid receptor (GR) as a potential molecular target of XXXD treatment. Collectively, these findings demonstrated that XXXD reduced adiposity, improved glucose tolerance, and restored insulin sensitivity through the suppression of inflammation in the NLRP3-dependent signaling pathway.

DOI: https://doi.org/10.35702/diab.1007

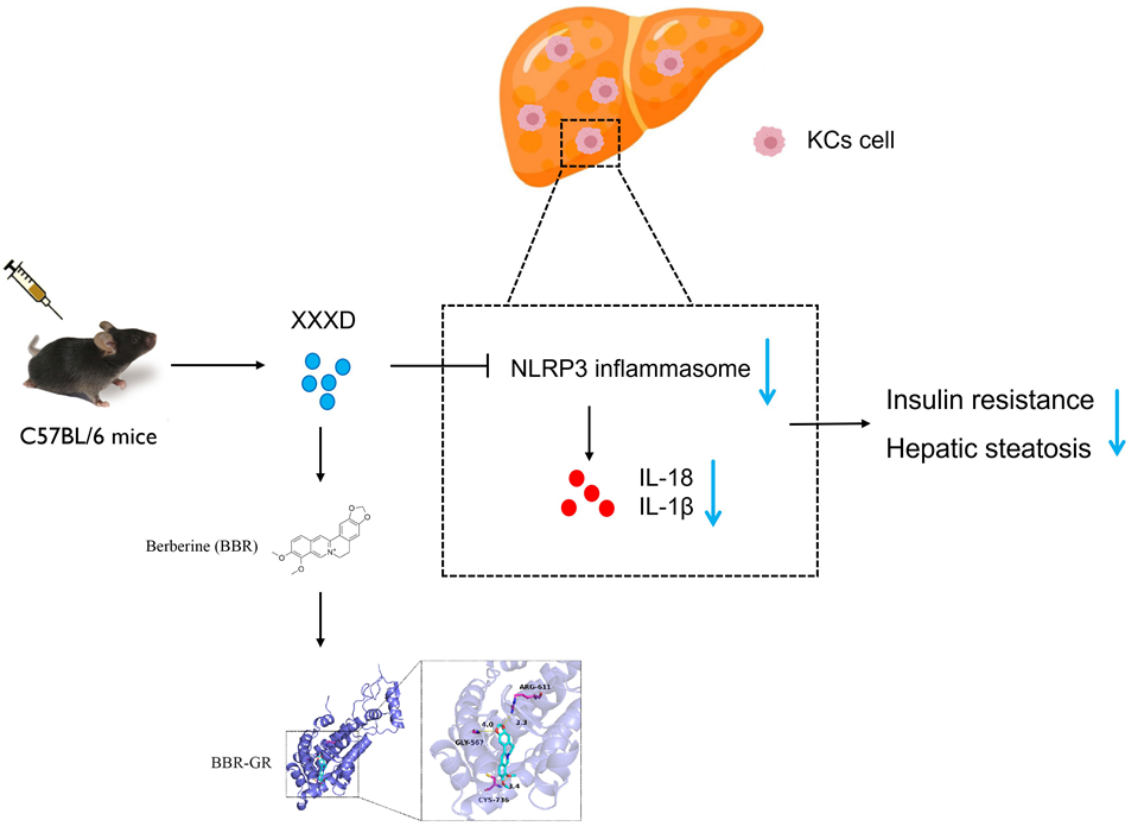

Keywords: Xiaoxianxiong Decoction, Type 2 diabetes, Glucose Tolerance, Inflammation, NLRP3

INTRODUCTION

Obesity leads to chronic and systemic inflammation, resulting in insulin resistance (IR), impaired insulin secretion, glucose intolerance, and type 2 diabetes (T2D) [1]. In this regard, chronic tissue inflammation has emerged as a key feature of obesity and T2D and is observed in insulin target tissues, such as adipose tissue and the liver. The key component of inflammatory activation is a multimeric protein complex termed the inflammasome, which is activated by cell nutrients, such as glucose and free fatty acids, inducing inflammatory cytokine interleukin-1 beta (IL-1β) production [2]. IL-1β is derived from NLRP3 inflammasomes in pro-inflammatory macrophages. This macrophage-derived IL-1β impairs insulin secretion and decreases insulin signaling, contributing to the development of glucose intolerance and T2D [3,4].

Xiaoxianxiong decoction (XXXD) is a classic and well-known decoction that is used to treat coronary heart disease or reduce phlegm and clear heat in clinical for a long time [5]. It is worth noting that XXXD has also been used to treat patients with severe pneumonia exhibiting symptoms such as abnormal breathing, depression, fever, and cough [6]. Mechanistically, XXXD protects against LPS-induced pneumonia by inhibiting the inflammatory response through activating SIRT1 [7]. Furthermore, berberine, the main compound in XXXD, has been proven to reduce pulmonary inflammation in mice by preventing gasdermin D-mediated pyroptosis and NLRP3 inflammasome activation [8]. The glucocorticoid receptor (GR), a target receptor of glucocorticoids (GCs), plays a vital role in controlling the expression of various inflammatory genes [9]. Previous reports have shown that GR activation can orchestrate the regulation of conventional NLRP3-inflammasome activation through its actions as a transcription factor on the Nlrp3 mRNA level. For this reason, it is a major nuclear receptor drug target for the treatment of inflammatory disorders. However, the role of XXXD as an effective formula in ameliorating obesity-induced T2D is poorly understood.

MATERIALS AND METHODS

Preparation of Xiaoxianxiong Decoction (XXXD)

XXXD is composed of Huanglain (Coptidis Rhizoma), Banxia (Arum Ternatum, unb.), and Gualou (Trichosanthes Kirilowii Maxim). The herbs were purchased from TCM Pharmacy of

Guang'anmen Hospital of China Academy of Chinese Medical Sciences (Beijing, China). All medicinal plants were decocted 30 min twice with boiling deionized water (1:10 and then 1:5, w/v). After filtering, the solution was concentrated using a rotary vacuum evaporator (70°C) to 1.5 g raw herbs/mL

Animals

All mice were housed and maintained under specific-pathogen-free (SPF) conditions at the Department of Laboratory Animal Science of Peking University Health Science Center. All animal experiments were performed according to protocols approved by the Ethics Committee of Peking University Health Science Center.

For C57BL/6 mice, six-week-old male mice were placed on a HFD (60% kcal from fat; D12492, Research Diets, USA) or a normal chow diet until the end of the experimental protocol. After exposure for 8 weeks to the respective diets, the HFD-fed mice were injected intraperitoneally with 40 mg/kg streptozotocin (STZ) solution after overnight fasting for 5 consecutive days. The chow group received the vehicle only. The HFD + STZ mice were administered 0.9% sodium chloride (HFD group), 75 mg/kg Metformin (Met group), 6.7 g/kg XXXD (XL group), 16.75 g/kg XXXD (XM group), and 26.8 g/kg XXXD (XH group) daily for 8 weeks.

Mice were euthanized after 8 weeks of treatment, and then the liver tissues were collected. The tissues were cut into small pieces, and then frozen in liquid nitrogen or fixed in 10% formalin for further analyses or processed for histology below.

Histology

Liver tissues excised from the mice were fixed in 10% neutral buffered formalin. The tissues were then paraffin-embedded, 4 μm sections prepared, and subjected to hematoxylin and eosin (H&E) staining. Pulmonary metastases were identified by microscopic analyses of H&E-stained sections.

Oil Red O

Lipid deposition in the livers was assessed by oil red O staining, while the morphology of livers was observed after HE staining. Briefly, the intact aortas were fixed in 4% paraformaldehyde for 48 h. The liver sections were stained with 0.5% oil red O solution (Servicebio, G1015, Wuhan, China) for 1 h, and then differentiated in a 60% propylene glycol solution for 5 min. The stained livers were photographed on an optical microscope (Carl Zeiss, Germany). The percentage of Oil Red O-stained areas in rat liver sections was analyzed by ImageJ. The method for the quantification of the Oil Red O-stained area was performed as described previously [10].

Cell Culture

The HepG2 cells were obtained from the American Type Culture Collection (ATCC) and cultured in Dulbecco's Modified Eagle's Medium (DMEM) with 1% penicillin/streptomycin and 10% fetal bovine serum (FBS) (Invitrogen, USA) at 37 °C in a humidified atmosphere with 5% CO2. A reported method with minor modifications was used to develop an IR cell model by culturing HepG2 cells in serum-free DMEM containing 25 mM glucose and 2 μg/mL insulin (Solarbio, Beijing, China) for 36 h. XXXD was dissolved in dimethyl sulfoxide (DMSO), and the final concentration of DMSO in each well was 0.1 %. Metformin (J&K Scientific, Beijing, China) was used as a positive control.

Flow Cytometry

Liver perfusion was performed as described previously (Liu et al., 2017; Mederacke et al., 2015). Briefly, mice were anesthetized, and livers were perfused via portal vein catheterization successively with pre-warmed Hank's balanced salt solution (HBSS) containing 1 mM ethylene glycolbis (aminoethylether)-tetra-acetic acid (EGTA), 40 μg/ml Liberase (Sigma-Aldrich, USA), and 5 mM CaCl2. After perfusion, livers were removed, gently disassociated with forceps in Dulbecco's modified Eagle's medium (DMEM) (Gibco, USA) containing 5% FBS, and filtered through a 70 μm cell strainer. The nonparenchymal cells were isolated via centrifuging at 50 g for 3 min followed by 350 g for 6 min at 4°C, and subjected to red blood cell lysis. Cells were incubated with anti-mouse CD16/CD32 mAb (BD Biosciences, USA) for 5 min at 4°C and then with fluorophore-conjugated antibodies or isotype controls for an additional 30 min. The antibodies used were as follows: PE/Cyanine7-conjugated anti-CD86 (105013, BioLegend, USA), PE-conjugated anti-F4/80 (123109, BioLegend, USA), FITC-conjugated anti-CD11b (101205, BioLegend, USA), and APC-conjugated CD206 (MMR) (141707, BioLegend, USA). After incubation with antibodies, cells were washed twice. All data were acquired using a BD LSRFortessa flow cytometer (BD Bioscience) and analyzed with FlowJo software.

Quantitative Real-Time PCR

To measure mRNA levels, total RNA was isolated from cells or tissues using TRIzol reagent according to the manufacturer's protocol. The isolated mRNA was reverse-transcribed into

cDNA using HiScript III All-in-one RT SuperMix (QP018, abm). Real-time PCR reactions were prepared with Taq Pro Universal SYBR qPCR Master Mix (Vazyme) and then analyzed using an Applied Biosystems 7500. mRNA expression levels of target genes were normalized to those of GAPDH mRNA. The primer pairs used for the PCR experiments are listed in Supplemental Table S1.

Western Blot

Total protein was extracted using a RIPA lysis buffer supplemented with a protease/phosphatase inhibitor cocktail. Protein concentrations were measured using a Bicinchoninic Acid (BCA) Assay Kit. Equal amounts of protein were resolved on a 10% SDS-polyacrylamide gel electrophoresis gel and then electrotransferred to a polyvinylidene difluoride (PVDF) membrane. The following antibodies were used to probe for the proteins of interest: anti-rabbit NLRP3 (catalog no. 30109-1-AP, Proteintech), anti-rabbit ASC (catalog no. 67824, Cell Signal Technology), anti-rabbit caspase-1 (catalog no. 31020-1-AP, Proteintech), and anti-rabbit GAPDH (catalog no. 2118S, clone 14C10, Cell Signaling Technology) was used as a loading control. Signals were visualized with film using an enhanced chemiluminescence (ECL) prime western blotting system.

Molecular Docking

A molecular docking approach was used to analyze potential interactions between berberine (BBR) and the glucocorticoid receptor (GR). The crystal structures of the glucocorticoid receptor (PDB: 7PRX) were obtained from the RCSB Protein Data Bank (https://www.rcsb.org/), and the 3D structure of BBR was retrieved from the PubChem database. A binding conformation between the BBR and the GR was predicted by AutodockVina 1.2.2, a protein–ligand docking software. The binding energy (outcome of molecular docking) was used to assess the ligand–receptor binding. Finally, visualization of the molecular interaction between BBR and glucocorticoid receptor was performed using Autodock Vina 1.2.2 (http://autodock.scripps.edu/).

Molecular dynamics (MD) simulations

MD simulations were carried out with Desmond/Maestro noncommercial version 2022.1 software. TIP3P water molecules were added to the systems, which were then neutralized by 0.15 M NaCl solution. After minimization and relaxation of the system, the production simulation was performed for 200 ns in an isothermal-isobaric ensemble at 300 K and 1 bar. Trajectory coordinates were recorded every 200 ps. The MD analysis was performed using a simulation interaction diagram from Desmond.

Statistical analysis

All statistical analyses were performed using Prism GraphPad software v8.0.2. To assess differences between two groups, a two-tailed unpaired Student's t-test was used. Differences were considered significant when $p < 0.05$, *$**p < 0.01$, $***p < 0.001$, and $****P < 0.0001$*. Experimental results are typically presented as means ± SEM, unless otherwise stated.

RESULTS

Generation of type 2 diabetes (T2D) Mice

To test the effect of the XXXD on the pathogenesis of obesity, we first generated T2D mouse models by HFD feeding and multiple low-dose STZ injections. The body weights were recorded to assess obesity. At 8 weeks of HFD and STZ injections, the body weights of mice increased to 36.64 ± 2.20 g compared to 29.54 ± 1.18 g in the chow-fed mice (Figure 1A). The blood glucose levels of mice were also significantly higher than those of the chow-fed mice (Figure 1B). T2D mice showed significant impaired glucose tolerance, as indicated by the Oral glucose tolerance test (OGTT) and area under the curve during the OGTT (Figure 1C). Reduced insulin sensitivity was also observed in those mice as measured by the insulin tolerance test (ITT) and area above the curve during the ITT (Figure 1D).

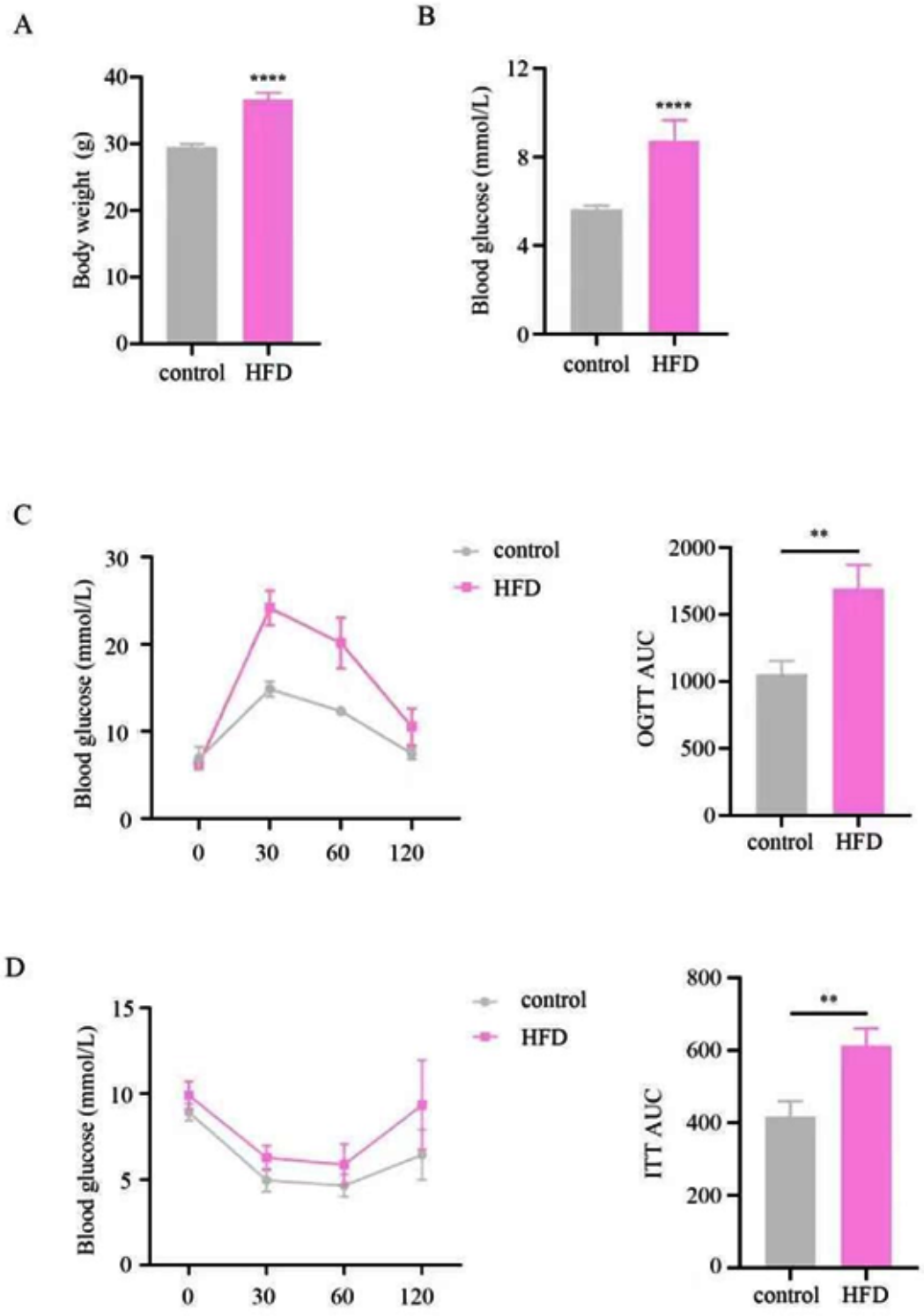

Figure 1: Generation of T2D mouse model by HFD feeding and STZ injection

A. Changes in body weights in C57BL/6 mice fed with normal chow (n=10) or high-fat diet with STZ (T2D, n = 50). Bars represent means ± SD. *****p < 0.0001.*

B. Random (non-fasting) blood glucose levels in C57BL/6 mice fed with normal chow (n=10) or high-fat diet with STZ injection (n=50). Bars represent means ± SEM. *****p < 0.0001.*

C. Blood glucose levels and area under the curve in chow and T2D mice during the OGTT. Bars represent means ± SEM. ***p < 0.01.*

D. Blood glucose levels and area above the curve during the ITT in chow and T2D mice. Bars represent means ± SEM. ***p < 0.01.*

Citation: Ding R, et al. (2026). Xiaoxianxiong Decoction Ameliorates Obesity-induced Type 2 Diabetes by Suppressing the NLRP3 Inflammasome Activation. Diabetes Research. 3(1):07.

DOI: https://doi.org/10.35702/diab.1007

Xiaoxianxiong decoction alleviates insulin resistance, hyperlipidemia, and hepatic steatosis

HFD feeding can induce insulin resistance, liver steatosis, and modest inflammation. After treatment with XXXD for 8 weeks, XXXD-treated mice had significantly lower blood glucose levels, indicative of elevated gluconeogenesis, compared with the T2D controls (Figure 2A). Consistent with the insulin resistance (IR) phenotype, basal insulin levels were significantly downregulated in XXXD-treated mice, compared with the controls fed the same diet (Figure 2B). The body weights of XXXD-treated mice significantly decreased compared to the T2D mice (Figure 2C). Compared to the HFD-induced T2D mice, the XXXD groups improved glucose tolerance and insulin sensitivity (Figure 2D and 2E).

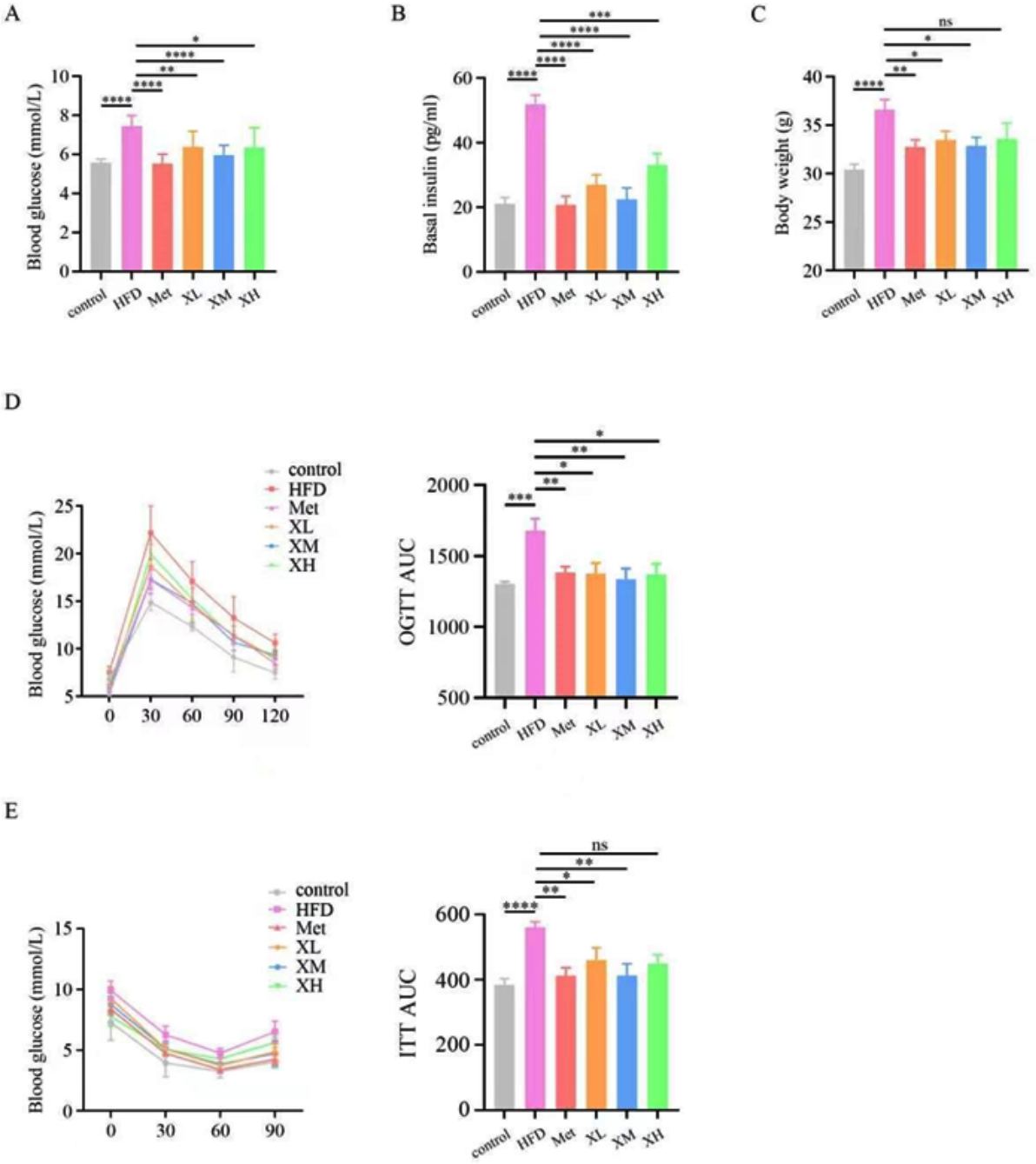

Figure 2: The effects of Xiaoxianxiong decoction (XXXD) on insulin resistance

DOI: https://doi.org/10.35702/diab.1007

A. Non-fasting blood glucose levels in chow-fed mice and T2D mice treated with saline (HFD), Metformin (Met, 75 mg/kg), low dose of XXXD (XL, 6.7 mg/kg), medium dose of XXXD (XM, 16.75 mg/kg), and high dose of XXXD (XH, 26.8 mg/kg). Bars represent means ± SEM (n = 8). *****p < 0.0001, **p < 0.01, *p < 0.05.*

B. Basal insulin levels of chow-fed and T2D mice treated daily with Met and XXXD as in Panel A. Data points are means ± SEM (n = 8). *****p < 0.0001, **p < 0.01.*

C. Body weights of chow-fed and T2D mice treated daily as in Panel A. Data points are means ± SEM (n = 8). *****p < 0.0001, **p < 0.01. *p < 0.05, NS, p > 0.05.*

D. (D and E) OGTT (D) and ITT (E) were performed and quantified as area under the curve (AUC), respectively. *****p < 0.0001, ***p < 0.001, **p < 0.01, *p < 0.05, NS, p > 0.05.*

In addition to the effects of XXXD treatment on improved glucose homeostasis, we also found that XXXD suppressed the concentration-independent increase in neutral lipid droplets in T2D mice compared with the control (Figure 3A). The hepatocytes in XXXD-treated mice were complete and clear, with few lesions. Oil red O staining demonstrated obvious lipid deposition in the liver of T2D mice, while XXXD attenuated Oil red O-positive scope (Figure 3B). This observation was further confirmed in the IR-HepG2 modeling (Figure 3C). As shown in Supplemental Figure 1, the intervention with insulin in HepG2 cells significantly decreased the consumption of extracellular glucose but recovered by XXXD treatment compared with the control group. The XXXD extract was nontoxic to HepG2 at the concentrations of 1, 10, and 100 μg/ml after 24 h incubation. Additionally, the total triglycerides (TG) and low-density lipoprotein cholesterol (LDL-C) decreased significantly in XXXD-treated mice (Figure 3D and 3E). These data demonstrated that XXXD treatment had the capability to ameliorate IR, hyperlipidemia, and obesity in HFD-induced T2D mice. These results suggest that XXXD treatment had a striking protective effect against the development of hepatic steatosis in the HFD-fed mice, resulting in a significant decrease in liver TGs.

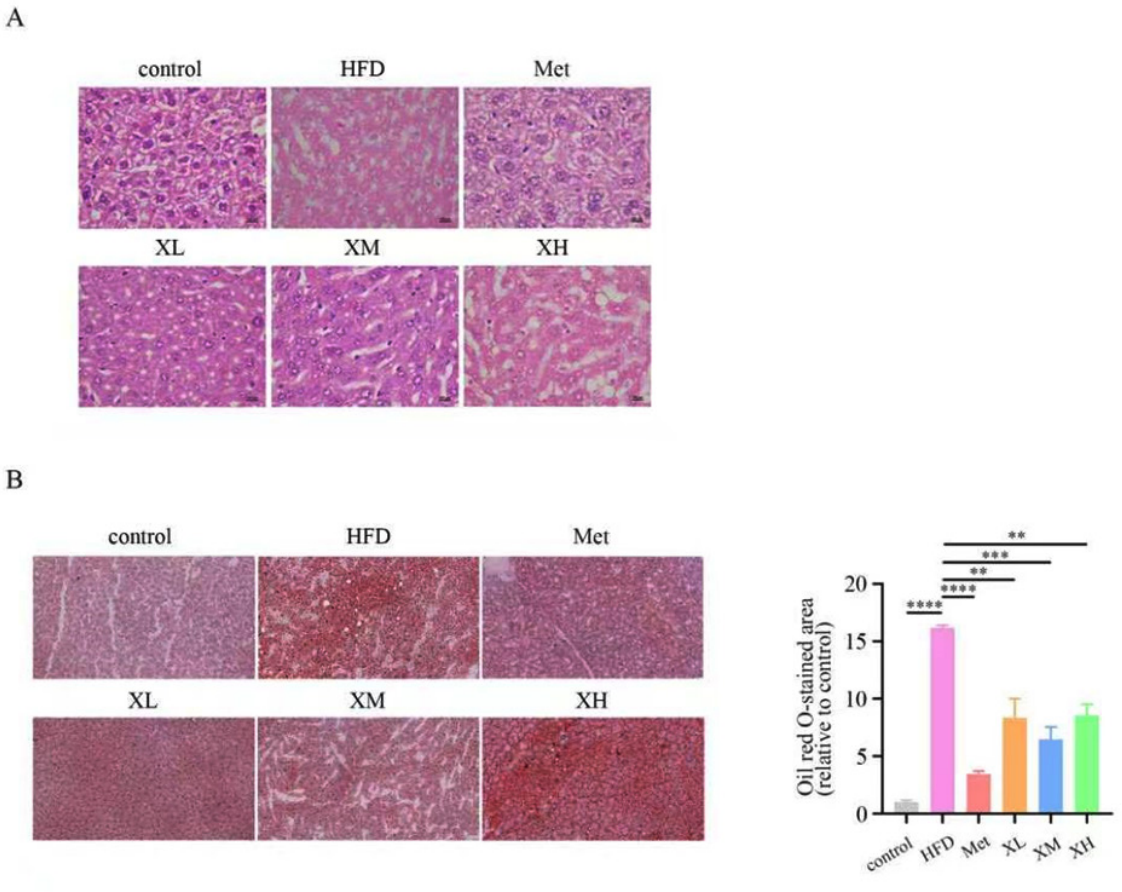

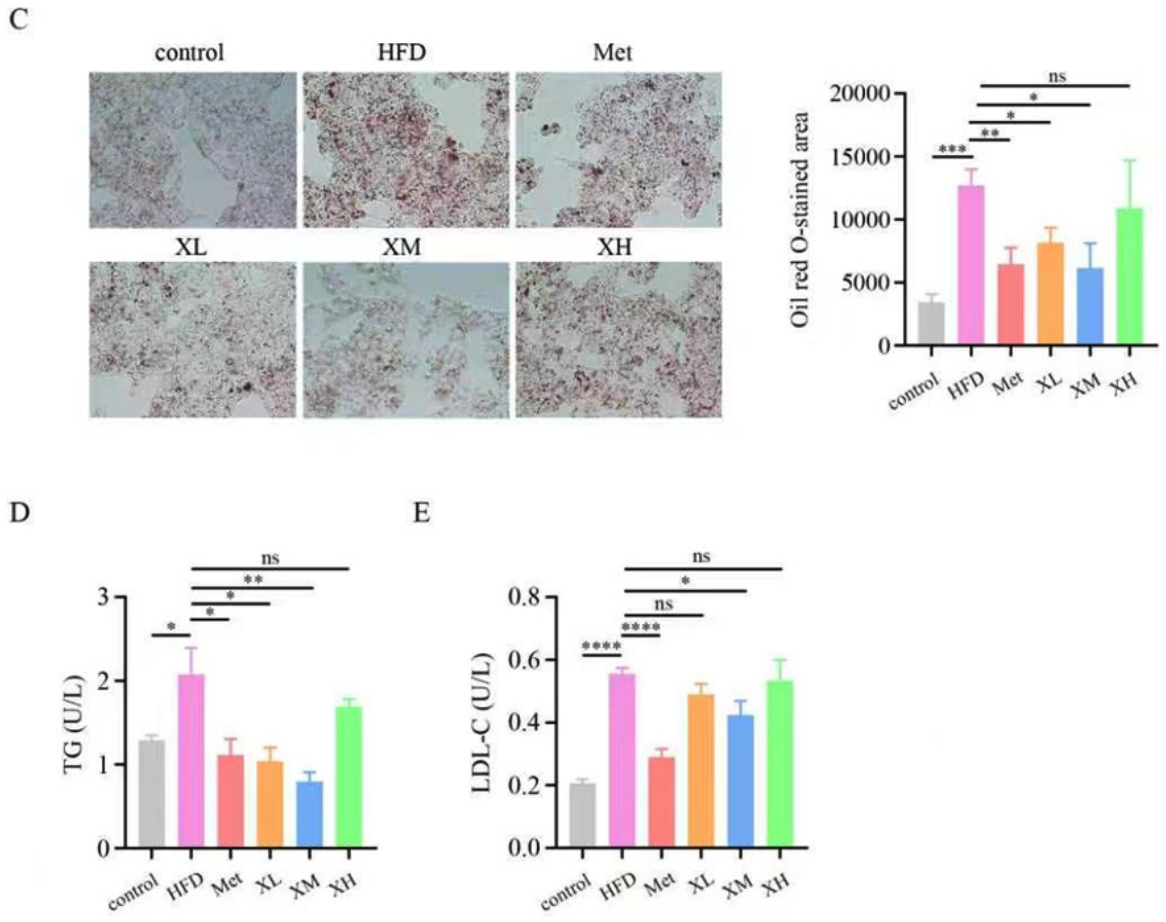

Figure 3: XXXD treatment protects against hepatic steatosis in HFD-fed mice

A. Representative images of H&E staining of liver tissues from T2D mice treated with saline (HFD), Metformin (Met, 75 mg/kg), low dose of XXXD (XL, 6.7 g/kg), medium dose of XXXD (XM, 16.75 g/kg), and high dose of XXXD (XH, 26.8 g/kg). Scale bar, 100 μm.

B. Evaluation of lipid droplets in liver tissues by Oil Red O staining after XXXD administration. Scale bar =100 μm. The percentage of Oil Red O-stained areas in rat liver sections was analyzed by Image J. *****p < 0.0001, **p < 0.01*.

C. The cells were treated with either 1 mM Metformin or 1-100 μg/ml XXXD for 24 h. The effect of XXXD on lipid accumulation was assessed using Oil Red O staining, and the cells were photographed using a microscope. Scale bar, 100 μm. Data points are means ± SEM (n = 3). ****p < 0.001, **p < 0.01. *p < 0.05, NS, p > 0.05.*

D. (D and E) The levels of serum TG (D) and LDL-C (E) exposed to XXXD were determined. Data points are means ± SEM (n = 8). *****p < 0.0001, **p < 0.01. *p < 0.05, NS, p > 0.05.*

XXXD suppresses hepatic inflammation and activation of the NLRP3 inflammasome

Inflammation in the liver can cause hepatic steatosis and reduce insulin sensitivity [1]. As previously reported, HFD plus STZ upregulates proinflammatory genes and macrophage infiltration [11]. We showed an upregulation of various inflammatory markers after 8 weeks of HFD feeding, including proinflammatory cytokines interleukin-1β (IL1β) and interleukin-18 (IL-18) (Figure 4A). NLRP3 inflammasome activation leads to maturation and secretion of proinflammatory cytokines interleukin-1β (IL1β), which is involved in the inflammatory response[12]. To test the effect of XXXD on NLRP3 inflammasome activation, qRT-PCR and immunoblotting assays were performed to determine the expression of NLRP3, adapter protein apoptosis-associated speck-like protein (ASC), and caspase-1 in livers from T2D mice. As shown in Figure 4B and 4C, XXXD treatment significantly suppressed these gene expressions at both the mRNA and protein levels. These results suggested that XXXD suppressed hepatic inflammation through the NLRP3-mediated signaling pathway.

ISSN: 2998-4920

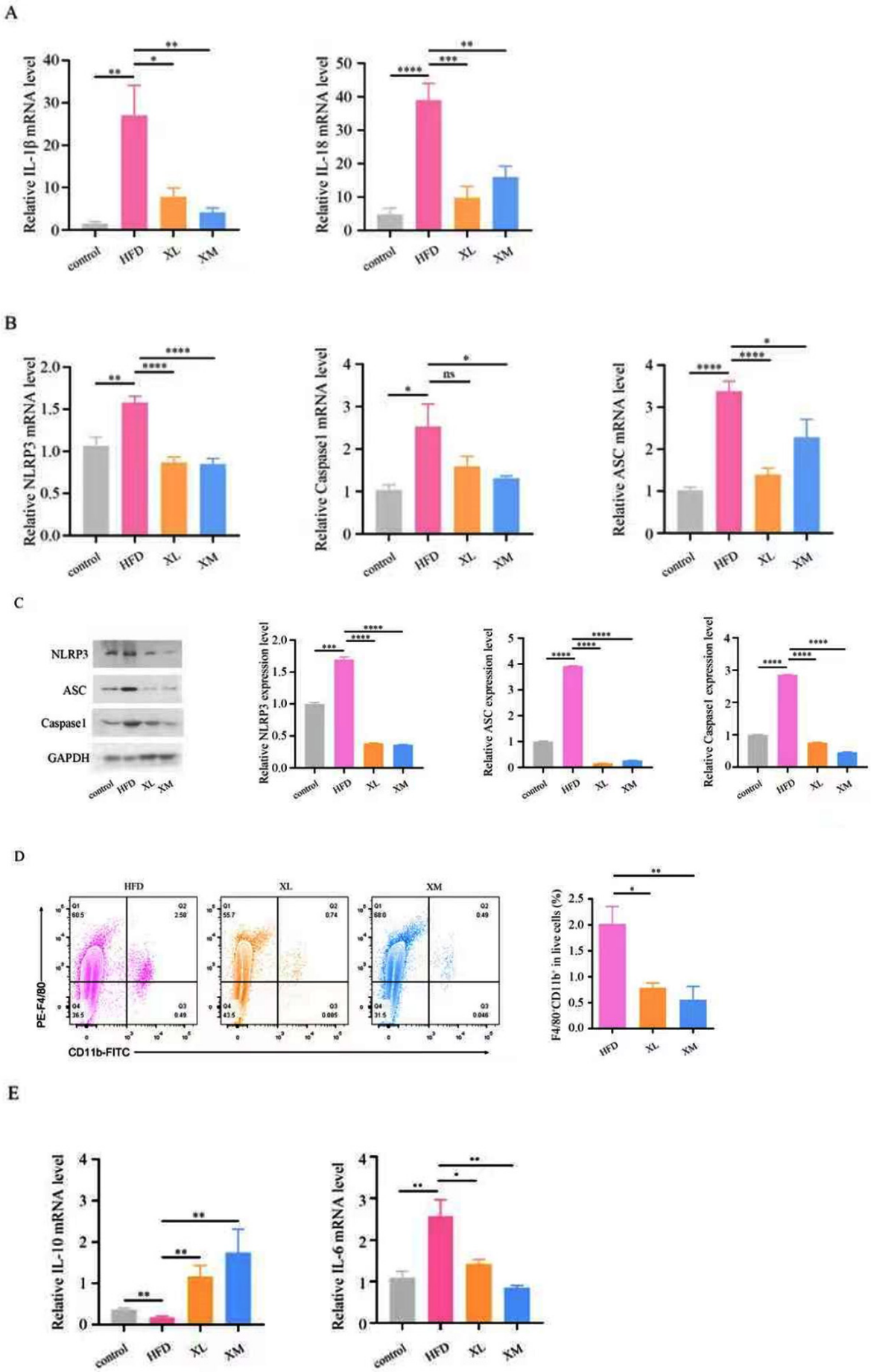

Figure 4: XXXD suppresses hepatic inflammation and activation of the NLRP3 inflammasome

DOI: https://doi.org/10.35702/diab.1007

A. Relative mRNA levels of IL-1β and IL-18 in liver tissues of saline (HFD), low dose of XXXD (XL, 6.7 g/kg), and medium dose of XXXD (XM, 16.75 g/kg)-treated T2D mice. Data shown are means ± SEM (n = 3). ****p < 0.0001, *****p < 0.001, **p < 0.01. *p < 0.05.*

B. Relative mRNA levels of NLRP3, ASC, and caspase-1 in liver tissues of T2D mice treated with low dose of XXXD (XL, 6.7 g/kg), medium dose of XXXD (XM, 16.75 g/kg), or saline (HFD) were analyzed by qRT-PCR. Data shown are means ± SEM (n = 3). *****p < 0.0001, **p < 0.01. *p < 0.05, NS, p > 0.05.*

C. Immunoblot analysis of NLRP3, ASC, and caspase-1 levels in livers from T2D mice treated with low dose of XXXD (XL, 6.7 g/kg), medium dose of XXXD (XM, 16.75 g/kg), or saline (HFD), quantitated by densitometry. Bars represent means ± SEM. *****p < 0.0001.*

D. Flow cytometric analysis of KCs (F4/80+CD11b+) in liver tissues from T2D mice treated with saline (HFD), low dose of XXXD (XL, 6.7 g/kg), or medium dose of XXXD (XM, 16.75 g/kg). Data in the bar graph (right panel) are presented as means ± SEM, n = 8. **p < 0.01, *p < 0.05.*

E. Relative IL-10 and IL-6 mRNA levels in livers from T2D mice treated daily as in Panel A. Data shown are means ± SEM (n = 3). **p < 0.01, *p < 0.05.*

XXXD alleviates macrophage infiltration and activation in T2D liver

It has been well established that macrophages have a central role in innate immunity, but they also play a part in the coordination of metabolic inflammation linked to metabolic diseases, including obesity and T2D [13]. As a major metabolic organ, the liver comprises two macrophage populations: Kupffer cells (KCs), the resident specialized hepatic macrophage, and monocyte-derived macrophages (MoMFs), the recruited macrophages arising from circulating monocytes. Under overnutrition conditions, activated pro-inflammatory KCs initiate the inflammation and induce the infiltration of MoMFs, which display a highly pro-inflammatory phenotype and lead to IR as well as hepatic steatosis through NLRP3 [14,15]. In this study, we intended to unveil XXXD effects on the HFD-induced T2D model. We proceeded to elucidate whether XXXD influences the liver macrophages, in particular, the infiltration of KCs (F4/80+CD11b+). Flow cytometric analysis further demonstrated that the number of KCs was decreased in the XXXD-treated mice compared to HFD-induced T2D mice (Figure 4D), suggesting that the infiltration of KCs was significantly inhibited by XXXD treatment. In addition to heterogeneity of developmental origins, hepatic macrophages also display plasticity in polarization, ranging from a pro-inflammatory phenotype (M1) to an anti-inflammatory state (M2) [16]. M1 macrophages, characterized by the production of pro-inflammatory cytokines, contribute to obesity-induced IR and hepatic steatosis, while M2 macrophages exert ameliorative effects [17,18]. As shown in Figure 4E, T2D mice showed higher mRNA expression levels of M1 markers, including IL1β and IL6, whereas the expression of M2 marker, IL10, was downregulated in liver tissues. Remarkably, XXXD treatment in the T2D mice resulted in the downregulation of IL1β and IL6 in the livers (Figure 4E). These results indicate that XXXD inhibits T2D-induced macrophage activation in the liver. Collectively, the chronic inflammatory environment of the T2D liver has been improved.

Identification of glucocorticoid receptor (GR) as a potential molecular target of XXXD treatment

XXXD is composed of Huanglain (*Coptidis Rhizoma*), Banxia (*Arum Ternatum Thunb*), and Gualou (*Trichosanthes Kirilowii Maxim*). The chemical profiles of XXXD were established by liquid chromatography mass spectrometry ion trap/time of flight (LCMS-IT-TOF) mass spectrometer in positive-ion mode. The results showed berberine (BBR) as the main compound in XXXD (Supplemental Figure 3). The BBR has garnered considerable attention for its broad-spectrum biological activities, including anti-diabetic, anti-obesity activities, and anti-inflammatory [19]. The glucose-lowering effect of BBR has been validated in both animal experiments and human clinical trials. In addition, BBR markedly decreased serum pro-inflammatory cytokines IL-17 and TNF-α levels [20]. The glucocorticoid receptor (GR) is a major nuclear receptor drug target for the treatment of inflammatory disorders [21]. It can interact with proinflammatory transcription factors, such as NF-κB, AP-1, and STAT, to repress their transcriptional activity [22,23]. To elucidate the mechanism underlying ameliorated obesity-induced IR and inflammation following treatment with XXXD, we conducted a molecular docking simulation using AutoDock Vina software to predict the putative BBR binding site on GR (PDB: 7PRX). The results showed that BBR has a high affinity for GR with a docking energy of -8.5 kcal/mol (Figure 5A). Computational methods suggest that BBR forms hydrogen bonds with Gly567, Arg611, and Cys736 of GR, which could anchor BBR well in the protein binding pocket. MD simulations were then employed to evaluate the stability of BBR binding to GR. As shown in Figure 5B, the finding suggests a direct, high-affinity binding of BBR to GR, providing a structural basis for direct regulation of insulin resistance.

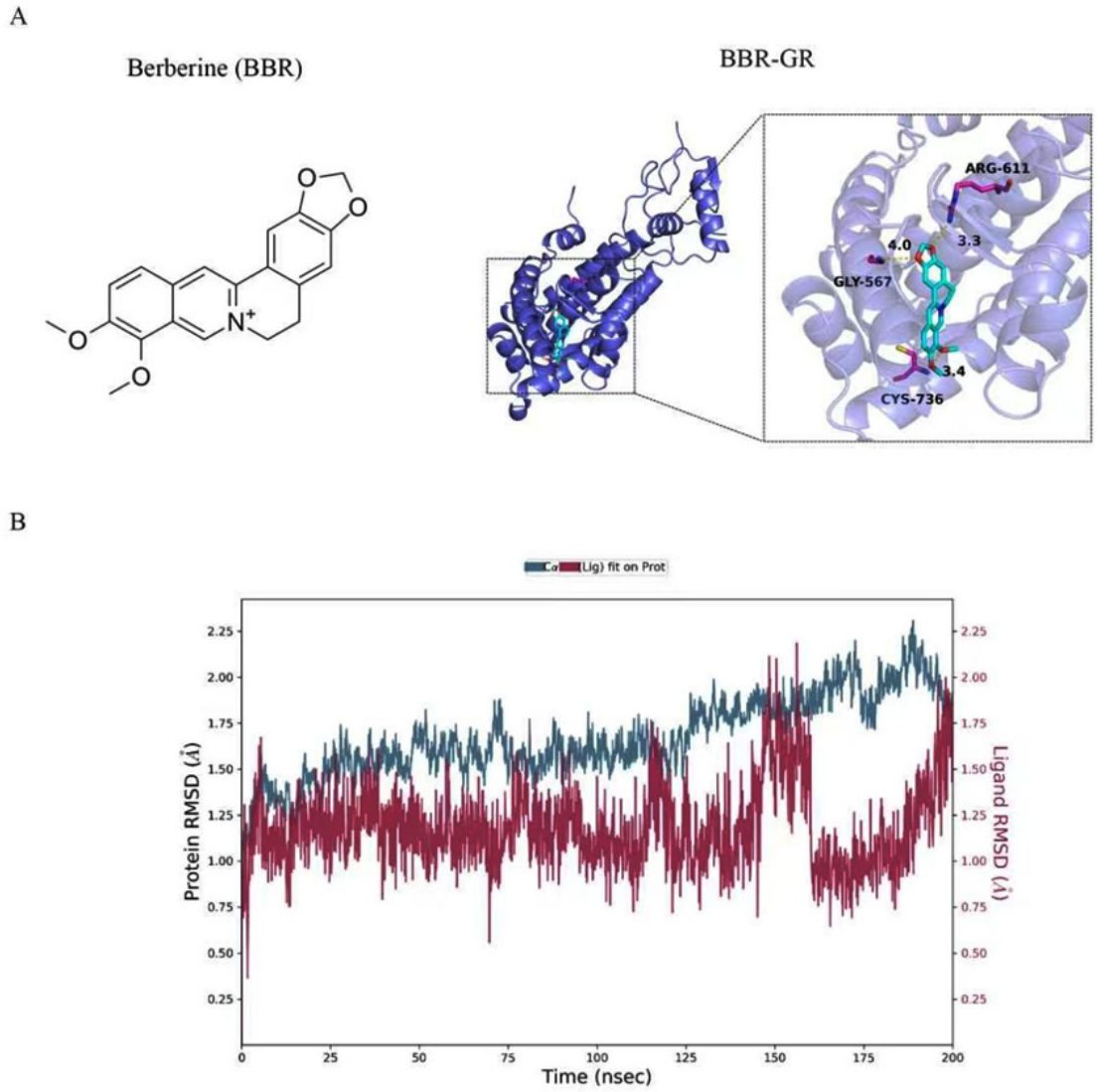

Figure 5: Berberine potentially directly targets the glucocorticoid receptor

A. Structure of glucocorticoid receptor (GR) showing a hypothetical binding pocket of Berberine (BBR) (light blue). Computational simulations suggest BBR forms hydrogen bonds with Gly567, Arg611, and Cys736 of GR.

B. Profiles of molecular dynamics simulations: root mean square deviations (RMSD) of BBR (red) and GR residues (blue).

DISCUSSION

Obesity characteristically leads to hepatic steatosis and liver inflammation [24]. The potential contribution of chronic tissue inflammation to metabolic disease has been suggested for many years [25,26]. Adipose tissue in obesity expresses high levels of pro-inflammatory cytokines TNF-α, and its neutralization improves insulin sensitivity and glucose intolerance [27]. Another prominently released cytokine, IL-1β, impairs adipocyte insulin signaling in adipose tissue [4]. Thus, targeting inflammation could be a therapeutic approach for the treatment of metabolic disease. XXXD is a widely used clinical prescription effective in the treatment of pneumonia. It protects against LPS-induced pneumonia by inhibiting the inflammatory response through the activation of SIRT1. However, the potential of XXXD to improve obesity-induced insulin resistance and T2D requires further investigation. In this study, we found that XXXD alleviated insulin resistance in T2D mice. Along with its effects on improved glucose homeostasis, XXXD also protects against the development of hepatic steatosis.

NLRP3 inflammasome has a central role in obesity induced inflammation, IR, and T2DM [28]. NLRP3 interacts with ASC, which binds to procaspase-1, forming the NLRP3 inflammasome [29,30]. This process leads to procaspase-1 self-cleavage, generating the active caspase-1, which induces the conversion of IL-1β immature forms to active forms that

are secreted [31]. Our results showed that XXXD treatment significantly suppressed the expression of NLRP3, ASC, and caspase-1 at both the mRNA and protein levels. These results suggested that XXXD suppressed obesity-induced inflammation, IR, and T2DM through inactivation of NLRP3 inflammasome.

Innate immune cells in the liver are mainly KCs, which are the most abundant tissue-resident macrophages. KCs play a crucial role in regulating hepatic lipid metabolism and hepatic steatosis. Selective ablation of KCs significantly improved hepatic insulin resistance and alterations of hepatic insulin signaling. This indicates that KCs are important in the initiation mechanism of high-fat diet-induced hepatic insulin resistance. Additionally, activated KCs can aggravate hepatic inflammation [32,33]. They are the primary source of IL-1β production, which mainly occurs through the activation of NLRP3 inflammasomes [34], suggesting that KCs facilitate the increased NLRP3 expression. Our flow cytometric analysis demonstrated that the percentage of KCs was significantly downregulated, indicating that XXXD treatment significantly inhibited KCs infiltration. It has been reported that KCs were activated and aggravated inflammatory injury in hepatic steatosis through the NLRP3 pathway. This inflammatory injury in hepatic steatosis increased the secretion of inflammatory factors such as TNF-α and IL-1β. The activation of NLRP3 in KCs represents a key mechanism in inflammatory injury associated with hepatic steatosis. Our data provide evidence that targeting of the NLRP3 inflammasome in KCs could be a potential therapeutic approach for the improvement of obesity-induced T2D.

The whole-herb decoctions, such as XXXD decoction, contain multiple active compounds; these active constituents are often unknown and variable. This makes it difficult to determine which molecule is responsible for a therapeutic effect. The composition of decoctions can differ based on factors such as plant species or subspecies, soil conditions, harvest timing, storage methods, and extraction method. Two batches of the "same" decoction may differ substantially in composition and potency. Herbal decoctions rarely provide precise concentrations of active constituents. To understand the mechanism underlying XXXD suppressing the NLRP3 inflammasome activation, we screened the berberine (BBR), the main compound in XXXD, for further investigation. BBR has been demonstrated to reduce pulmonary inflammation in mice with influenza virus pneumonia by preventing NLRP3 inflammasome activation [35]. It inhibits the activation of the NF-κB/NLRP3 signaling pathway and directly blocks NLRP3 protein [36,37]. Previous reports have shown that GR activation is important for regulating the NLRP3 signaling pathway [38,39]. The activation of GR in enterocyte cells can attenuate the expression of NLRP3 to exert intestinal barrier protective effects [40]. In this study, we found that BBR may directly bind to GR with high affinity, providing a structural basis for direct regulation of NLRP3 inflammasome activation.

CONCLUSIONS

In conclusion, our findings strongly support that XXXD not only reduces adiposity and enhances glucose tolerance but also restores insulin sensitivity by suppressing inflammation through the NLRP3-dependent signaling pathway. This innovative approach presents a significant advancement in the treatment of T2D, paving the way for future therapeutic strategies.

ACKNOWLEDGEMENTS

We thank Jingjing Gong from Peking University Health Science Center for helpful discussions for this study.

FUNDING

This work is supported by the grants to Z.Z. including the Clinical Research Center Construction Project of Guang'anmen Hospital, CACMS (grant no. 2022LYJSZX24), the Special Fund for the Training of Newly Recruited Young Researchers, Basic Scientific Research Operating Expenses, China Academy of Chinese Medical Sciences (grant no. ZZ18-XRZ-082).

DATA AVAILABILITY STATEMENT

All data needed to evaluate the conclusions in the paper are present in the paper and/or the Supplementary Materials.

AUTHOR CONTRIBUTIONS STATEMENT

Z. Zhang and R. Ding conceptualized the project and designed the experiments. Methodology and investigations were done by R. Ding, Y. Wang, and Y. Yang analyzed the data. R. Ding, Y. Wang, and Z. Zhang wrote and revised the manuscript.

ETHICAL APPROVAL AND CONSENT TO PARTICIPATE

All animal experiments were performed according to protocols approved by the Ethics Committee of Peking University Health Science Center.

CONFLICT OF INTEREST

The authors declare that they have no competing interests.

REFERENCES

1. Rohm TV, Meier DT, Olefsky JM, Donath MY. (2022). Inflammation in obesity, diabetes, and related disorders. Immunity. 11;55(1):31-55.

2. Böni-Schnetzler M, Boller S, Debray S, Bouzakri K, Meier DT, Prazak R, et al. (2009). Free fatty acids induce a proinflammatory response in islets via the abundantly expressed interleukin-1 receptor I. Endocrinology. 150(12):5218-5229.

3. Eguchi K, Manabe I, Oishi-Tanaka Y, Ohsugi M, Kono N, Ogata F, et al. (2012). Saturated fatty acid and TLR signaling link β cell dysfunction and islet inflammation, Cell Metabolism. 15(4):518-533.

4. Maedler K, Sergeev P, Ris F, Oberholzer J, Joller-Jemelka HI, Spinas GA, et al. (2002). Glucose-induced beta cell production of IL-1beta contributes to glucotoxicity in human pancreatic islets, J Clin Invest. 110(6):851-860.

5. Lu XH, Li J. (2021). Classical Chinese Herbal Formulas in the Treatment of Coronary Heart Disease: A Narrative Review. Chinese Journal of Integrative Medicine. 27(1):70-79.

6. Zhang G, Li Q, Zhang J. (2025). Clinical Effects of Traditional Chinese Medicine + Azithromycin in the Treatment of Mycoplasma Pneumonia, International Journal of General Medicine. 18:825–833.

7. Shi L, Zhang J, Cai Y, Bao J, Chen H. (2025). Xiaoxianxiong Decoction Attenuates LPS-Induced Pneumonia in Mice by Inhibiting Inflammatory Response Through Activation of SIRT1. FASEB Bioadv. 7(10):e70060.

8. An C, Wu Y, Wu J, Liu H, Zhou S, Ge D, et al. (2022) Berberine ameliorates pulmonary inflammation in mice with influenza viral pneumonia by inhibiting NLRP3 inflammasome activation and gasdermin D-mediated pyroptosis, Drug Development Research. 83(7):1707-1721.

9. Zhan X, Song B, Xu S, Zhou H. (2026) Glucocorticoid receptor signaling: crosstalk with inflammation. Immunopharmacology and immunotoxicology. 48(1):67-78.

10. Nishad A, Naseem A, Rani S, Malik S. (2023) Automated qualitative batch measurement of lipid droplets in the liver of bird using ImageJ. STAR Protoc. 15;4(3):102466.

11. Cao M, Pan Q, Dong H, Yuan X, Li Y, Sun Z, Dong X, Wang H. (2015) Adipose-derived mesenchymal stem cells improve glucose homeostasis in high-fat diet-induced obese mice, Stem Cell Research & Therapy. 6:208.

12. Vande Walle L, Lamkanfi M. (2023). Drugging the NLRP3 inflammasome: from signalling mechanisms to therapeutic targets. Nature reviews. Drug discovery. 23(1):43-66.

13. Christopher KG, Jerrold MO. (2012). Inflammation and lipid signaling in the etiology of insulin resistance, Cell metabolism. 15(5):635-645.

14. Kazankov K, Jørgensen SMD, Thomsen KL, Møller HJ, Vilstrup H, George J, et al. (2018). The role of macrophages in nonalcoholic fatty liver disease and nonalcoholic steatohepatitis, Nature Reviews. Gastroenterology & Hepatology. 16(3):145-159.

15. Lee YS, Wollam J, Olefsky JM. (2018). An Integrated View of Immunometabolism, Cell. 172(1-2):22-40.

16. Bai X, Guo YR, Zhao ZM, Li XY, Dai DQ, Zhang JK, et al. (2025)., Macrophage polarization in cancer and beyond: from inflammatory signaling pathways to potential therapeutic strategies. 625:217772.

17. Zhu M, Cheng Y, Zuo L, Bin B, Shen H, Meng T, et al. (2024). siRNA-loaded folic acid-modified TPGS alleviate MASH via targeting ER stress sensor XBP1 and reprogramming macrophages. 20(10):3823-3841.

18. Lin XF, Cui XN, Yang J, Jiang YF, Wei TJ, Xia L, et al. (2024) SGLT2 inhibitors ameliorate NAFLD in mice via downregulating PFKFB3, suppressing glycolysis and modulating macrophage polarization. 45(12):2579-2597.

19. Chen G, Zhang C, Zou J, Zhou Z, Zhang J, Yan Y, et al. (2025). Coptidis rhizoma and berberine as anti-cancer drugs: A 10-year updates and future perspectives, Pharmacol Res. 216:107742.

20. Yang T, Ma X, Wang R, Liu H, Wei S, Jing M, et al. (2022). Berberine inhibits IFN-γ signaling pathway in DSS-induced ulcerative colitis, Saudi Pharm J. 30(6):764-778.

21. Clarisse D, Van Moortel L, Van Leene C, Gevaert K, De Bosscher K. (2024). Glucocorticoid receptor signaling: intricacies and therapeutic opportunities. Trends in Biochemical Sciences. 49(5):431-444.

22. Reichardt HM, Kaestner KH, Tuckermann J, Kretz O, Wessely O, Bock R, et al. (1998). DNA binding of the glucocorticoid receptor is not essential for survival, Cell. 93(4):531-541.

23. Hyun-June Y, Hi-Joon P, Bombi L, Dae-Hyun HJJIR. (2025). The Bidirectional Interaction Between NF-κB and Glucocorticoid Receptor: Underlying Mechanisms of Chronic Stress-Induced Pathology.

24. Stergios AP, Jannis K, Christos SM. (2018). Obesity and nonalcoholic fatty liver disease: From pathophysiology to therapeutics, Metabolism. 92:82-97.

25. Cook DG, Mendall MA, Whincup PH, Carey IM, Ballam L, Morris JE, et al. (2000) C-reactive protein concentration in children: relationship to adiposity and other cardiovascular risk factors, Atherosclerosis. 149(1):139-50.

26. Esser N, Legrand-Poels S, Piette J, Scheen AJ, Paquot N. (2014). Inflammation as a link between obesity, metabolic syndrome and type 2 diabetes, Diabetes Research and Clinical Practice. 105(2):141-150.

27. Vila-Bedmar R, Cruces-Sande M, Lucas E, Willemen HL, Heijnen CJ, Kavelaars A, et al. (2015) Reversal of diet-induced obesity and insulin resistance by inducible genetic ablation of GRK2, Sci Signal. 21;8(386):ra73.

28. Qiang M. (2023). Pharmacological Inhibition of the NLRP3 Inflammasome: Structure, Molecular Activation, and Inhibitor-NLRP3 Interaction, Pharmacological Reviews. 75(3):487-520.

29. Shao BZ, Xu ZQ, Han BZ, Su DF, Liu C. (2015). NLRP3 inflammasome and its inhibitors: a review. Frontiers In Pharmacology. 6:262.

30. Cabral JE, Wu A, Zhou H, Pham MA, Lin S, McNulty R. (2025). Targeting the NLRP3 inflammasome for inflammatory disease therapy. Trends in Pharmacological Sciences. 46(6):503-519.

31. Davis BK, Wen H, Ting JP. (2011). The inflammasome NLRs in immunity, inflammation, and associated diseases, Annual Review of Immunology. 29:707-735.

32. Xu H, Li H, Woo SL, Kim SM, Shende VR, Neuendorff N, et al. (2014). Myeloid cell-specific disruption of Period1 and Period2 exacerbates diet-induced inflammation and insulin resistance, The Journal of Biological Chemistry. 289(23):16374-16388.

33. Cai Y, Li H, Liu M, Pei Y, Zheng J, Zhou J, et al. (2018) Disruption of adenosine 2A receptor exacerbates NAFLD through increasing inflammatory responses and SREBP1c activity, Hepatology. 68(1):48-61.

34. Li P, He K, Li J, Liu Z, Gong J. (2017). The role of Kupffer cells in hepatic diseases, Molecular Immunology. 85:222-229.

35. Fan Y, Wang J, Feng Z, Cao K, Xu H, Liu J. (2020) Pinitol attenuates LPS-induced pneumonia in experimental animals: Possible role via inhibition of the TLR-4 and NF-κB/IκBα signaling cascade pathway. Journal of Biochemical and Molecular Toxicology. 35(1):e22622.

36. Jiyu, C., Yanli, H., Xiaohong, B. & Yan, H. J. F. N. (2022). Berberine Ameliorates Inflammation in Acute Lung Injury via NF-κB/Nlrp3 Signaling Pathway. 9:851255.

37. Yin W, Pengfei D, Donghui JJPD. (2020). Berberine functions as a negative regulator in lipopolysaccharide -induced sepsis by suppressing NF-κB and IL-6 mediated STAT3 activation. 78.

38. Lucafò M, Granata S, Bonten EJ, McCorkle R, Stocco G, Caletti C, et al. (2021). Hypomethylation of NLRP3 gene promoter discriminates glucocorticoid-resistant from glucocorticoid-sensitive idiopathic nephrotic syndrome patients. Clinical and Translational Science. 14(3):964-975.

39. Zhao Q, Wu CS, Fang Y, Qian Y, Wang H, Fan YC. (2019). Glucocorticoid Regulates NLRP3 in Acute-On-Chronic Hepatitis B Liver Failure. 16(3):461-469.

40. Cai L, Chen Q, Yao Z, Sun Q, Wu L, Ni Y. (2020). Glucocorticoid receptors involved in melatonin inhibiting cell apoptosis and NLRP3 inflammasome activation caused by bacterial toxin pyocyanin in colon. Free Radical Biology & Medicine. 162:478-489.

SUPPLEMENTARY MATERIALS AND METHODS

Glucose Consumption of IR-HepG2 Cells

The IR-HepG2 cell model was established as described above and treated with a series concentration of XXXD or Metformin. The glucose concentration in supernatant was measured using a glucose oxidase and peroxidase (GOD-POD) kit (TC0711, Leagene, China), and the consumption of glucose of each well was calculated by subtracting the glucose concentration in the wells with cells from that in the blank wells.

Liquid Chromatography Mass Spectrometry Ion Trap/Time of Flight Analysis

Liquid chromatography (LC) analyses were conducted on a HPLC system (Shimadzu, Kyoto, Japan) consisting of an LC-20AD binary pump, DGU-20A degasser, SIL-20A autosampler, CTO-20AC column oven, and SPD-M20A photodiode array (PDA) detector. The mobile phase (delivered at 1.0 ml/min) consisted of acetonitrile (A) and water containing 0.1% formic acid (B). The following gradient elution program was used: 0–30 min: 5% A–30% A, 30–70 min: 30% A–45% A, 70–90 min: 45% A–90% A. The samples were separated on a YMC-C18 column (5 μm, 4.6×250 mm, YMC Co. Ltd., Kyoto, Japan) equipped with a Zorbax SB-C18 guard column (5 μm, 4.6 ×12.5 mm, Agilent Technologies, Waldbronn, Germany). The column temperature was 30˚C. Shanghai Bide Pharmatech Co. Ltd. provided the reference standard for berberine (purity > 98%). The concentration of XXXD used for HPLC analysis was 1 g/mL (1 mL solution contains 1 g of the original herbs). A liquid chromatography mass spectrometry ion trap/time of flight (LCMS-IT-TOF) mass spectrometer (Shimadzu) was equipped with an Atmospheric pressure chemical ionization (APCI) source in positive and negative ion mode. For qualitative analysis, scan ranges were set at m/z 100-1000 for MS1 and 100-500 for MS2. Authentic berberine was handled under the same conditions.

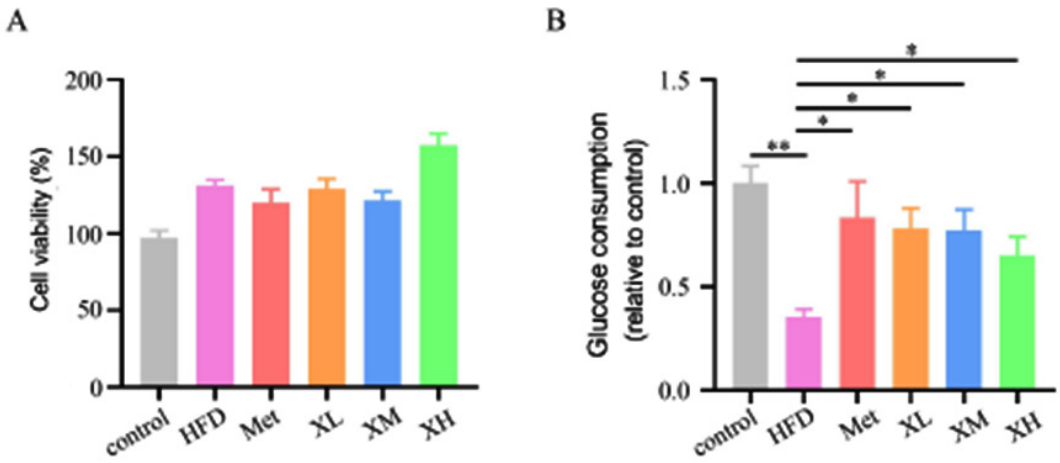

Supplemental Figure 1: (A) The impact of XXXD (from 1 to 100 μM) and Metformin on cell proliferation of IR-HepG2 cells was determined by MTT assay. **(B)** Glucose consumption in IR-HepG2 cells were detected with a glucose oxidase and peroxidase (GOD-POD) kit.

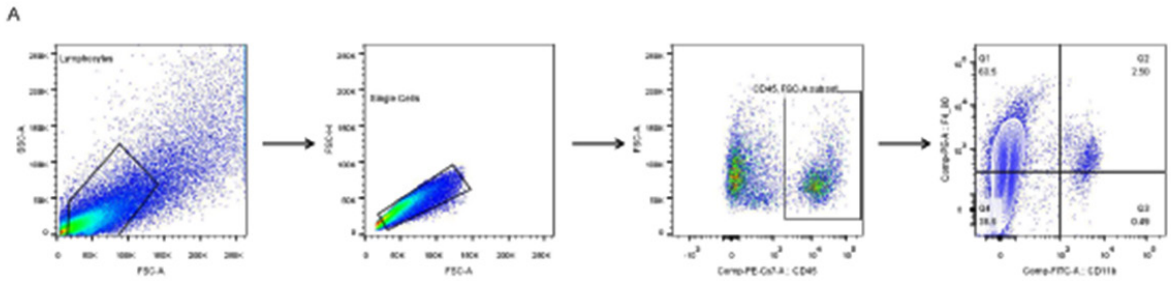

Supplemental Figure 2: (A) Flow cytometry gating strategy was employed to identify distinct subsets of macrophages within the liver tissues of mice.

ISSN: 2998-4920

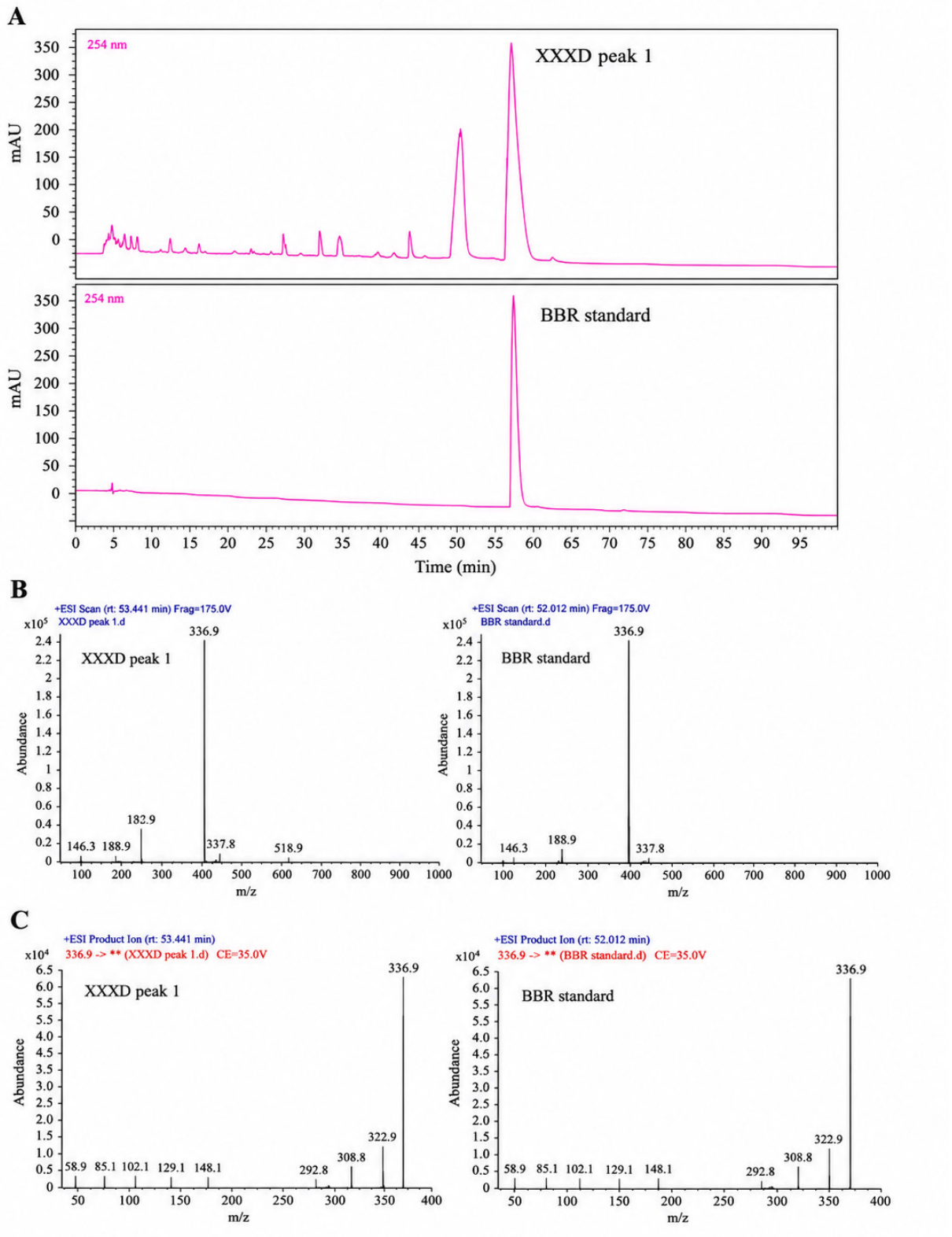

(A) The chromatogram of XXXD and authentic standard at 254 nm. Identified compound is BBR (Peaks 1; Rt = 35.57 min).
(B) The positive mass spectra of the main compound BBR (m/z = 336.12) from XXXD sample and the authentic standard.
(C) The MS/MS spectrum of BBR from XXXD sample and the authentic standard.

DOI: https://doi.org/10.35702/diab.1007

ISSN: 2998-4920

Supplemental Table S1: List of all the primers in qRT-PCR

Assay	Forward Primer	Reverse Primer
Nlrp3	TCGTCACCATGGGTTCTGGT	GGCTTAGGTCCACACAGAAAGT
Caspase-1	CTATGGACAAGGCACGGGAC	TCAGCTGATGGAGCTGATTGA
Asc	ACTGTGCTTAGAGACATGGGC	TGGTCCACAAAGTGTCCTGTT
Il-6	ACAAGTCCGGAGAGGAGACT	GAATTGCCATTGCACAACTCT
Il-10	CTTACTGACTGGCATGAGGATCA	GCAGCTCTAGGAGCATGTGG
Il-18	GACTCTTGCGTCAACTTCAAGG	CAGGCTGTCTTTTGTCAACGA
Il-1β	GAAATGCCACCTTTTGACAGTG	TGGATGCTCTCATCAGGACAG
Gapdh	ACCCTTAAGAGGGATGCTGC	CCCAATACGGCCAAATCCGT